Nonlinear exceptional-point lasing with ab initio Maxwell–Bloch theory

Aayushman Sinha, Adarsh Jadhao, Aditya Prakash, Atharva Arora, Devansh Satra, Jason Gomez

Abstract

We present a general analysis for finding and characterizing nonlinear exceptional point (EP) lasers above threshold using steady-state ab initio Maxwell–Bloch equations. For a system of coupled slabs, we show that a nonlinear EP is obtained for a given ratio between the external pumps in each resonator and that it is associated with a kink in the output power and lasing frequency, confirming coupled-mode theory predictions. Through numerical linear stability analysis, we confirm that the EP laser can be stable for a large enough inversion relaxation rate. We further show that the EP laser can be characterized by scattering a weak signal off the lasing cavity so that the scattering frequency spectrum exhibits a quartic divergence. Our approach can be applied to arbitrary scatterers with multi-level gain media.

1 Introduction

Exceptional points (EPs), inherent to non-Hermitian systems, have emerged as a critical focus in photonics due to their unique spectral and dynamical properties. These singularities, characterized by the coalescence of eigenvalues and eigenvectors, enable phenomena fundamentally distinct from their Hermitian counterparts. While EPs have been extensively studied in linear photonic systems, the nonlinear regime remains underexplored despite its significant implications for laser physics and device engineering.

In this report, we investigate nonlinear EPs in lasing systems using the steady-state ab initio Maxwell–Bloch equations. Building upon prior theoretical predictions and experimental validations, we extend the analysis to reveal the interplay between nonlinear dynamics, gain saturation, and system stability at EPs. Our study encompasses coupled resonator systems, elucidating conditions for achieving nonlinear EPs above threshold and characterizing their impact on lasing output and spectral response. Furthermore, we propose an experimental framework for observing EP behavior through scattering analysis, showcasing potential applications in high-sensitivity sensing and nonlinear optical devices.

2 Coupled Mode Theory

For two coupled resonators with nonlinear gain saturation, steady state solutions can be described by:

$$\begin{bmatrix} i(G_1-\kappa_1) & g \\ g & i(G_1-\kappa_1) \end{bmatrix} \begin{bmatrix} \psi_1 \\ \psi_2 \end{bmatrix} = \Delta \begin{bmatrix} \psi_1 \\ \psi_2 \end{bmatrix} \tag{1}$$

where Δ is the relative frequency, g is a coupling rate, κ is a loss rate, $G_n = D_n/(1+|\psi|^2)$ is a gain rate that depends on the external pump D_n and the field amplitude ψ_n. We define $X_n = G_n - \kappa_n$. Solutions of the problem satisfy

$$2\Delta = i(X_1+X_2) \pm \sqrt{4g^2-(X_1-X_2)^2},\ |\psi_n|^2 = \frac{D_n}{\kappa_n+X_n} - 1,\ \psi_n(iX_n-\Delta)+g\psi_m = 0 \quad (n \neq m) \tag{2}$$

Lasing solutions require a real Δ. Two types of solutions are possible. First, for $X_1+X_2=0$ and $|X_1| \leq g$, we have real $\Delta = \pm\sqrt{g^2-{X_1}^2}$. At threshold, we have $\psi_n = 0$, so $D_1^{\text{th}} + D_2^{\text{th}} = \kappa_1+\kappa_2$. We call these PT-symmetric solutions since loss and gain are balanced between the two resonators ($X_1 = -X_2$). The second type is for $\Delta = 0$, which requires $X_1X_2 + g^2 = 0$. (We call these PT-broken solutions since the gain/loss balance is lost.) When such a condition holds, there is another purely imaginary solution $\Delta = i(X_1 - g^2/X_1)$. The stability of the system ($\text{Im}(\Delta) \leq 0$) requires $X_1 \leq g^2/X_1$ (i.e., $X_1 \leq -g$ or $0 \leq X_1 \leq g$). At threshold, these modes satisfy $(D_1^{\text{th}}-\kappa_1)(D_2^{\text{th}}-\kappa_2)+g^2 = 0$. The previous solutions are directly determined by the value of X_1. For each type of solutions, X_1 can be found using:

$$\frac{D_2}{\kappa_2+X_2} - 1 = |\psi_2|^2 = |\Delta - \frac{iX_1}{g}\psi_1|^2 = \frac{{X_1}^2+\Delta^2}{g^2}\left(\frac{D_1}{\kappa_1+X_1}-1\right) \tag{3}$$

For PT-symmetric solutions, Eq. (S3) simplifies to

$$X_1 = \frac{\kappa_2D_1-\kappa_1D_2}{D_1+D_2},\ |\psi_1|^2 = |\psi_2|^2 = \frac{D_1+D_2}{\kappa_1+\kappa_2} - 1,\ \Delta = \pm\sqrt{g^2 - \left|\frac{\kappa_2D_1-\kappa_1D_2}{D_1+D_2}\right|^2} \tag{4}$$

For PT-broken solutions, Eq. (3) is more complicated, but still gives a direct formula for D_2 as a function of X_1.
It is important to note that, for the previous solutions to be above threshold, we need $|\psi_1| > 0$, or equivalently $D_1/(\kappa_1 + X_1) > 1$.
An exceptional point is obtained at the boundary between the two types of solutions. This occurs for $X_1 = -X_2 = \pm g$ and $\Delta = 0$. Plugging in Eq. (S3) gives the condition for an exceptional point:

$$D_2 = \left(\frac{\kappa_2 \mp g}{\kappa_1 \pm g}\right) D_1. \tag{5}$$

This requires $\kappa_1 \geq g$ or $\kappa_2 \geq g$. Each of the two corresponding exceptional points is above threshold (lasing) when $D_1 \geq \kappa_1 \pm g$. One way to obtain the exceptional point is to first increase D_1 to a fixed value larger than $\kappa_1 \pm g$, then increase D_2 to the required value for the EP.

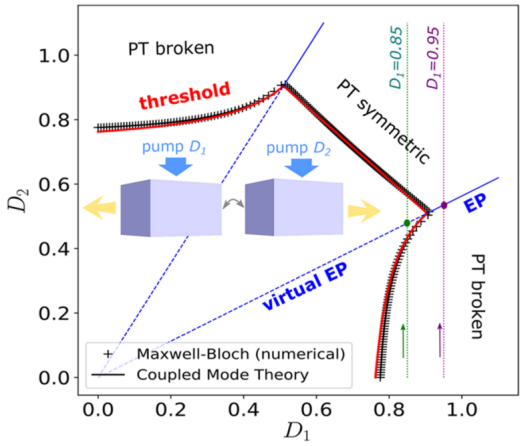

Figure 1: Phase diagram for a laser consisting of two coupled slabs with independent external pumps $D1$ and $D2$. The two-level gain medium inside the slabs is characterized by a central frequency $\frac{\omega_a}{2\pi c} = 1$ and linewidth $\frac{\gamma_a}{2\pi c} = 0.1$. Each slab has a refractive index $n_c = 3$, conductivity loss $\sigma_c = 0.5\omega_a$, and thickness $t = \frac{5a}{n_c}$, with an air gap $d \approx 0.2174a$, where a is an arbitrary unit length. '+' marker (respectively, red solid line) shows the numerical Maxwell–Bloch equation (respectively, CMT) threshold. A good fit is obtained using a loss factor $\kappa \approx 0.71$ and coupling coefficient $g \approx 0.2$. Blue solid (dashed) lines show the EP (virtual EP) as predicted by Eq. (4). Magenta (green) dotted line shows the pump path passing through the EP (Fig. 2).

- Two PT-symmetric modes coalesce at a single solution when $\kappa_{1,2} \geq g$.
- This coalescence results in a transition into the PT-broken phase with a lasing mode and an additional non-lasing solution (with complex Δ).
- The transition corresponds to a nonlinear Exceptional Point (EP) with:

$$\Delta_{EP} = 0 \text{ and } \psi_{EP} = e^{i\theta}\sqrt{\frac{D_1}{\kappa_1 \pm g} - 1}\begin{bmatrix} 1 \\ \mp g \end{bmatrix} \text{ (with arbitrary } \theta). \tag{6}$$

- The $\pm\pi/2$ phase difference between the amplitudes ψ_n indicates a chiral behavior.
- The two EPs are actual solutions only when $D_1 > \kappa_1 \pm g$.
- To obtain the EP, one can increase pump D_1 above the required value and then increase pump D_2 up to the value set by Eq. (4).
- It's possible to track the nonlinear EP along the line defined by Eq. (4) by simultaneously changing pumps D_1 and D_2.
- When the condition on D_1 is not satisfied, a virtual EP can be considered as a formal solution with negative intensity (i.e., $G_n = D_n/(1 - |\psi_n|^2)$).
- The virtual EP doesn't correspond to a physical solution but helps interpret the suppression and revival of lasing as a virtual nonlinear EP.

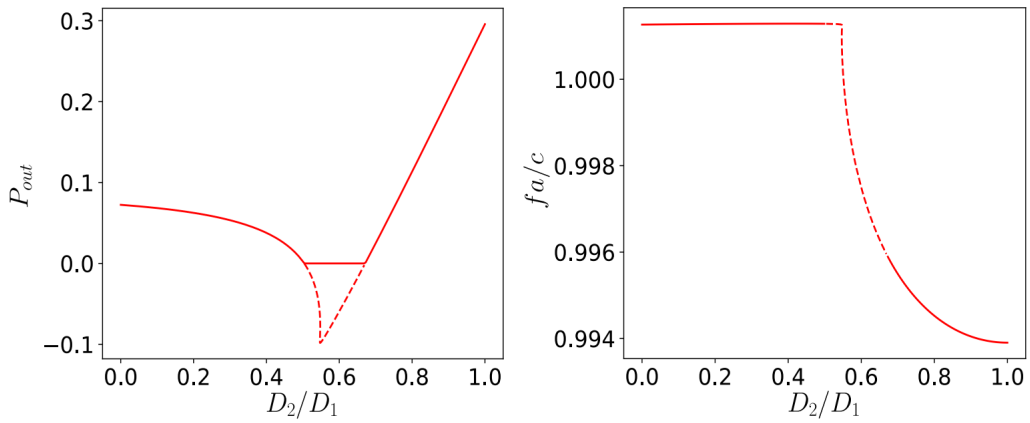

FIG. S2. Laser output power (left) and frequency (right) for a single-mode steady state solution of the nonlinear Maxwell-Bloch equation, by keeping the first slab pumped at $D_1 = 0.85$. Dashed lines represent formal numerical solution with a gain saturation $D_\ell = D_0/\left(1 + I_\ell|\Gamma_\ell E_\ell|^2\right)$ allowing I_ℓ to be negative. Physically, the laser shuts down when the power reaches zero (solid lines). At the lasing threshold the non-trivial negative intensity solution passes through the trivial non-lasing solution causing a bifurcation. This is true for any lasing mode and is not a special property of a mode at an EP [2].

We can also compute the output power of the laser as $P_{\text{out}} = \kappa_{1,r}|\psi_1|^2 + \kappa_{2,r}|\psi_2|^2$, where $\kappa_{n,r}$ is the radiative loss rate. For simplicity, we consider the case of equal losses between the two resonators ($\kappa_1 = \kappa_2$, $\kappa_{1,r} = \kappa_{2,r}$). For the PT-symmetric modes, we have

$$P_{\text{out}} = 2\kappa_r|\psi_1|^2 = \frac{\kappa_r}{\kappa}(D_1 + D_2) - 2\kappa_r \tag{7}$$

So the output power increases linearly with the pumps, with a rate $\partial P_{\text{out}}/\partial D_2 = \kappa_r/\kappa$. The dependence of P_{out} on the pumps is, however, more complicated for the PT-broken mode. We can still check that, at the EP, we have a discontinuity in the rate of P_{out} by explicitly computing $\partial P_{\text{out}}/\partial D_2$. After some algebra, we find for the PT-broken mode at the EP

$$\frac{\partial P_{\text{out}}}{\partial D_2} = \kappa_r \frac{\kappa D_1 - (\kappa \pm g)^2}{\kappa^2 D_1 - (\kappa^2 - g^2)(\kappa \pm g)} \tag{8}$$

We then have a discontinuity in $\frac{\partial P_{\text{out}}}{\partial D_2}$ at the EP. The largest discontinuity is obtained for the smallest possible D_1 (i.e., $\kappa \pm g$). In the limit of large D_1, there is no discontinuity, as Eq. (S7) goes to $\frac{\kappa_r}{\kappa}$ for $D_1 \to \infty$.
Our results here can also be used to interpret experiments in coupled photonic-crystal cavities. There, changing the position of the optical pump is equivalent to tuning D_2/D_1. But since the size of the pump-laser spot is large compared to the separation between the two cavities, D_2/D_1 could only be tuned slightly. With a graphene sheet used to partially cover one of the two cavities and increase its loss factor (equivalent to κ_2), the laser stays in the PT-symmetric phase for any positive pump value. With a large-area graphene sheet, κ_2 is large, giving a large EP-ratio D_2/D_1, so the laser remains in the PT-broken phase. Finally, a small-area graphene sheet gives an intermediate value for the EP-ratio D_2/D_1 allowing for the observation of an EP at the transition between the two phases by tuning the pump position.

2.1 Derivation of Output Power for PT Broken Solutions

From Eq. (3):

$$\frac{D_2}{\kappa_2 + X_2} - 1 = \frac{{X_1}^2 + \Delta^2}{g^2}\left(\frac{D_1}{\kappa_1 + X_1} - 1\right) \tag{2.1.1}$$

$$\Delta = 0,\ X_2 = -\frac{g^2}{X_1} \tag{2.1.2}$$

From Eq. (2.1.1), Eq.(2.1.2) and letting $\kappa_1 = \kappa_2 = \kappa$:

$$\implies \frac{D_2 X_1}{\kappa X_1 - g^2} - 1 = \frac{D_1 {X_1}^2}{g^2(\kappa + X_1)} - \frac{{X_1}^2}{g^2} \tag{2.1.3}$$

$$\implies \frac{(D_2 - \kappa)X_1 - g^2}{\kappa X_1 - g^2} = \frac{(D_1 - \kappa){X_1}^2 - {X_1}^3}{g^2(\kappa + X_1)} \tag{2.1.4}$$

Simplifying and writing the expression as a polynomial in X_1:

$$\implies \kappa {X_1}^4 - (g^2 + \kappa(D_1 - \kappa)){X_1}^3 + (g^2(D_1 + D_2 - 2\kappa)){X_1}^2 + (g^2(g^2 + \kappa(D_2 - \kappa)))X_1 + g^4\kappa = 0 \tag{2.1.5}$$

Here, $X_1(D_1, D_2)$ is basically a function that satisfies the above equation. Also, we know that at the EP, $X_1 = \pm g$, so we can obtain its derivatives with respect to D_1 and D_2 implicity.
Now, we also know:

$$|\psi_1|^2 = \frac{D_1}{X_1 + \kappa_1} - 1,\ |\psi_2|^2 = \frac{D_2}{X_2 + \kappa_2} - 1 \tag{2.1.6}$$

$$P_{out} = \kappa_r(|\psi_1|^2 + |\psi_2|^2) \quad (\text{Assuming } \kappa_{r,1} = \kappa_{r,2} = \kappa_r) \tag{2.1.7}$$

$$\implies P_{out}(D_1, D_2) = \kappa_r \left(\frac{D_1}{X_1(D_1, D_2) + \kappa} + \frac{D_2}{-g^2/X_1(D_1, D_2) + \kappa} - 2 \right) \tag{2.1.8}$$

$$\implies \frac{\partial P_{out}}{\partial D_2} = \kappa_r \left(\frac{-D_1}{(\pm g + \kappa)^2} \frac{\partial X_1}{\partial D_2}\bigg|_{EP} + \frac{-D_2}{(\kappa - g^2/\pm g)^2} \frac{\partial X_1}{\partial D_2}\bigg|_{EP} + \frac{1}{\kappa \mp g} \right) \tag{2.1.9}$$

$$\implies \frac{\partial P_{out}}{\partial D_2} = -\kappa_r \frac{\partial X_1}{\partial D_2}\bigg|_{EP} \left(\frac{D_1}{(\kappa \pm g)^2} + \frac{D_2}{(\kappa \mp g)^2} \right) + \frac{\kappa_r}{\kappa \mp g} \tag{2.1.10}$$

But at the EP, $D_2 = \left(\frac{\kappa_2 \mp g}{\kappa_1 \pm g}\right) D_1$. So, after substituting we get:

$$\implies \frac{\partial P_{out}}{\partial D_2} = -D_1 \kappa_r \frac{\partial X_1}{\partial D_2}\bigg|_{EP} \left(\frac{1}{(\kappa \pm g)^2} + \frac{1}{(\kappa^2 - g^2)} \right) + \frac{\kappa_r}{\kappa \mp g} \tag{2.1.11}$$

Now, to find $\frac{\partial X_1}{\partial D_2}\Big|_{EP}$, we partial differentiate Eq. (2.1.5) with respect to D_2:

$$\frac{\partial X_1}{\partial D_2} \left(4\kappa {X_1}^3 - 3(g^2 + \kappa(D_1 - \kappa)){X_1}^2 + 2g^2(D_1 + D_2 - 2\kappa)X_1 + g^2(g^2 + \kappa(D_2 - \kappa))\right) + g^2({X_1}^2 + X_1\kappa) = 0 \tag{2.1.12}$$

Now, since we need $\frac{\partial X_1}{\partial D_2}\Big|_{EP}$, we substitute X_1 at EP which is $X_1 = \pm g$:

$$\frac{\partial X_1}{\partial D_2}\bigg|_{EP} \left(\pm 4\kappa g^3 - 3(g^2 + \kappa(D_1 - \kappa))g^2 \pm 2g^2(D_1 + D_2 - 2\kappa)g + g^2(g^2 + \kappa(D_2 - \kappa))\right) + g^3(g \pm \kappa) = 0 \tag{2.1.13}$$

After using the fact that $D_2 = \left(\frac{\kappa \mp g}{\kappa \pm g}\right) D_1$ to eliminate D_2 and then simplifying the expression we get:

$$\frac{\partial X_1}{\partial D_2}\bigg|_{EP} \left(2(\kappa^2 - g^2) - 2\frac{k^2 D_1}{\kappa \pm g} \right) + g(g \pm \kappa) = 0 \tag{2.1.14}$$

Substituting value of $\frac{\partial X_1}{\partial D_2}\Big|_{EP}$ using Eq. (2.1.14) into Eq. (2.1.11) we get the following expression:

$$\implies \frac{\partial P_{out}}{\partial D_2} = -D_1 \kappa_r \left(\frac{1}{(\kappa \pm g)^2} + \frac{1}{(\kappa^2 - g^2)} \right) \left(\frac{g(g \pm \kappa)}{2\left(\frac{\kappa^2 D_1}{\kappa \pm g} - (\kappa^2 - g^2)\right)} \right) + \frac{\kappa_r}{\kappa \mp g} \tag{2.1.15}$$

After Simplifying the expression, we get the desired result which we mentioned in Eq. (2.1.15) above:

$$\frac{\partial P_{\text{out}}}{\partial D_2} = \kappa_r \frac{\kappa D_1 - (\kappa \pm g)^2}{\kappa^2 D_1 - (\kappa^2 - g^2)(\kappa \pm g)} \tag{2.1.16}$$

We then have a discontinuity in $\frac{\partial P_{\text{out}}}{\partial D_2}$ at the EP. The largest discontinuity is obtained for the smallest possible D_1 (i.e., $\kappa \pm g$). For $D_1 = \kappa \pm g$, we get $D_1 + D_2 = 2\kappa$ and from these two results we get that $\frac{\partial P_{out}}{\partial D_2} = \mp \kappa_r$

3 Linearised Maxwell-Bloch Equations

The previous coupled mode theory is a useful tool to obtain qualitative and semi-quantitative results, but it does not take into account other effects such as spatial mode profiles, spatially varying gain saturation, gain-medium line shape, and, importantly, gain medium dynamics, which can affect the stability of the system.
Here, we obtain numerical ab initio results within the framework of the semi-classical Maxwell–Bloch equations (with the rotating-wave approximation) that describe the interaction between the electromagnetic field and the gain medium modeled as a two-level system (for simplicity, written here assuming a single polarization):

$$\nabla^2 E^+ = \ddot{P}^+ + \epsilon_c \ddot{E}^+ + \sigma_c \dot{E}^+ \tag{9}$$

$$i\dot{P}^+ = (\omega_a - i\gamma_\perp)P^+ + \gamma_\perp E^+ D \tag{10}$$

$$\dot{D}/\gamma_\parallel = D_0 - D + \mathrm{Im}(E^{*+} \cdot P^+) \tag{11}$$

where E^+ is the positive-frequency component of the electric field (the physical field being given by $2\mathrm{Re}[E^+]$), P^+ is the positive-frequency polarization describing the transition between two energy levels (with frequency ω_a and linewidth $\gamma_\perp$), D is the population inversion (with relaxation rate $\gamma_\parallel$), D_0 is the pump strength profile, ϵ_c is the cold-cavity real permittivity, and σ_c is a cold-cavity conductivity loss. Here, we are assuming that the orientation of the atomic transition is parallel to the electric field, and we have written all three fields in their natural units.

The steady-state solution of these equations can be obtained via steady-state ab initio laser theory (SALT), which is exact (within the rotating wave approximation) for single-mode lasing and approximate for multi-mode lasing with well-separated modes. We use it to track single-mode lasing solutions as the external pump is changed by numerically solving the nonlinear steady-state equation:

$$\Theta E_\ell \equiv \left(\nabla^2 + \omega_\ell^2[\epsilon_c + i\frac{\sigma_c}{\omega_\ell} + \Gamma_\ell D_\ell]\right) E_\ell = 0, \tag{12}$$

where $\Gamma_\ell = \Gamma(\omega_\ell) \equiv \frac{\gamma_\perp}{\omega_\ell - \omega_a + i\gamma_\perp}$ and $D_\ell = \frac{D_0}{1+|\Gamma_\ell E_\ell|^2}$, with a corresponding polarization $P_\ell = \Gamma_\ell D_\ell E_\ell$.

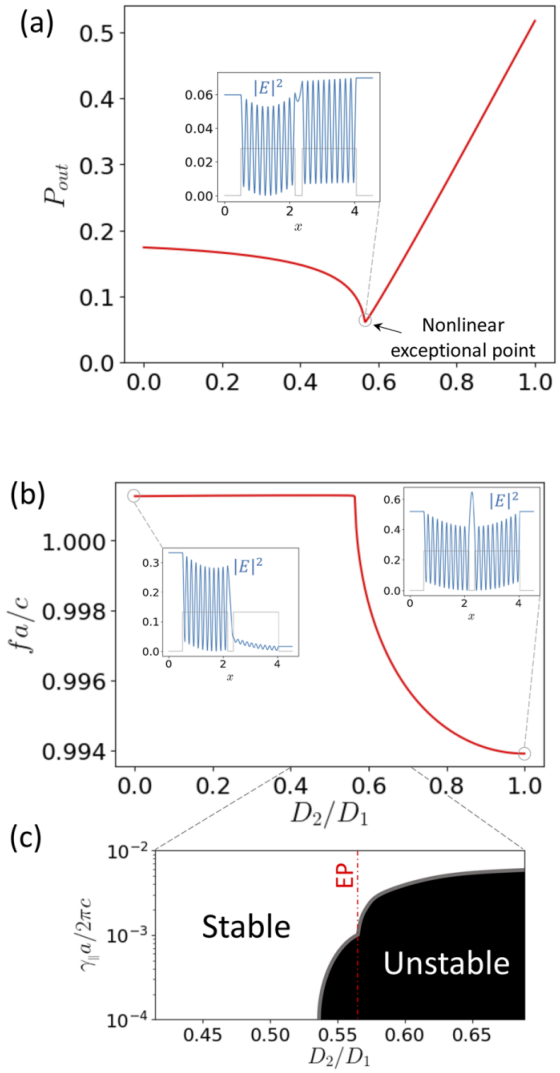

Figure 2: Output power (a) and frequency (b) for a single-mode steady-state solution of the nonlinear Maxwell–Bloch equation [Eq. (13)]. We pump the first slab until $D1 = 0.95$ (not shown in the plot) and then increase $D2$ (keeping $D1$ fixed). Insets show the mode intensity profile for different values of $D2$. (c) shows results of the numerical stability analysis. The nonlinear EP laser can be stable for large enough $\gamma_\parallel$.

3.1 Derivation of the Differential Equation

Maxwell-Bloch Equations, as mentioned above, with a current J are:

$$\nabla^2 E^+ = \ddot{P}^+ + \epsilon_c \ddot{E}^+ + \sigma_c \dot{E}^+ + \dot{J} \tag{3.1.1}$$

$$i\dot{P}^+ = (\omega_a - i\gamma_\perp)P^+ + \gamma_\perp E^+ D \tag{3.1.2}$$

$$\dot{D}/\gamma_\parallel = D_0 - D + \mathrm{Im}(E^{*+} \cdot P^+) \tag{3.1.3}$$

If the total Electric Field E is $E = \sum_\ell E_\ell e^{-i\omega_\ell t} + C \cdot C$ then $E^+ = \sum_\ell E_\ell e^{-i\omega_\ell t}$ (i.e. only the positive frequency component is considered). Same can be said for P.
For $J = 0$, first we derive Eq. (12) for a single-mode solution (which is considered to be an exact solution, according to the paper). So we take $E^+ = E_c e^{-i\omega_c t}$ and $P^+ = P_c e^{-i\omega_c t}$ and we substitute these into the above three Equations and respectively get:

$$\nabla^2 E_\ell = -{\omega_\ell}^2 P_\ell - \epsilon_c {\omega_\ell}^2 E_\ell - i\omega_\ell \sigma_c E_\ell \tag{3.1.4}$$

$$\omega_\ell P_\ell = (\omega_a - i\gamma_\perp)P_\ell + \gamma_\perp D E_\ell \implies (\omega_\ell - \omega_a + i\gamma_\perp)P_\ell = \gamma_\perp D E_\ell \tag{3.1.5}$$

$$D = D_0 + \mathrm{Im}(E_\ell^* \cdot P_\ell) \implies D = D_0 + \frac{1}{2i}(E_\ell^* \cdot P_\ell - E_\ell \cdot P_\ell^*) \tag{3.1.6}$$

To Simplify the Algebra, we take $T = \gamma_\perp/\Gamma_\ell$. Using Eqs. (3.1.5) and (3.1.6) we get,

$$TP_\ell = \gamma_\perp D_0 E_\ell + \frac{\gamma_\perp P_\ell |E_\ell|^2}{2i} - \frac{\gamma_\perp P_\ell^* {E_\ell}^2}{2i} \tag{3.1.7}$$

$$T^* P_\ell^* = \gamma_\perp D_0 E_\ell^* - \frac{\gamma_\perp P_\ell^* |E_\ell|^2}{2i} + \frac{\gamma_\perp P_\ell {E_\ell^*}^2}{2i} \implies \left(T^* + \frac{\gamma_\perp |E_\ell|^2}{2i}\right) P_\ell^* = \gamma_\perp E_\ell^* \left(D_0 + \frac{P_\ell E_\ell^*}{2i}\right) \tag{3.1.8}$$

Substituting P_ℓ^* using Eq. (3.1.7) in Eq. (3.1.8), we get:

$$TP_\ell = \gamma_\perp D_0 E_\ell + \frac{\gamma_\perp P_\ell |E_\ell|^2}{2i} - \frac{\gamma_\perp {E_\ell}^2}{2i} \left(\frac{\gamma_\perp E_\ell^* \left(D_0 + \frac{P_\ell E_\ell^*}{2i}\right)}{\left(T^* + \frac{\gamma_\perp |E_\ell|^2}{2i}\right)} \right) \tag{3.1.9}$$

Simplifying the expression, we get:

$$\left(|T|^2 + \frac{\gamma_\perp |E_\ell|^2 (T - T^*)}{2i}\right) P_\ell = \gamma_\perp D_0 E_\ell T^* \tag{3.1.10}$$

Now, Substituting back $T = \gamma_\perp/\Gamma_\ell$, we get the desired result after simplifying the expression:

$$P_\ell = \left(\frac{D_0}{1 + |\Gamma_\ell E_\ell|^2}\right) E_\ell \Gamma_\ell = D_\ell E_\ell \Gamma_\ell \tag{3.1.11}$$

From this equation we obviously get,

$$D_\ell = \left(\frac{D_0}{1 + |\Gamma_\ell E_\ell|^2}\right) \tag{3.1.12}$$

Now we also have from Eq. (3.1.4) and get the desired differential equation same as Eq. (12),

$$\nabla^2 E_\ell = -{\omega_\ell}^2 P_\ell - \epsilon_c {\omega_\ell}^2 E_\ell - i\omega_\ell \sigma_c E_\ell \implies \nabla^2 E_\ell = -{\omega_\ell}^2 \left(D_\ell E_\ell \Gamma_\ell + \epsilon_c E_\ell + \frac{i E_\ell \sigma_c}{\omega_\ell}\right) \tag{3.1.13}$$

$$\implies \Theta E_\ell \equiv \left(\nabla^2 + {\omega_\ell}^2 \left(D_\ell \Gamma_\ell + \epsilon_c + \frac{i\sigma_c}{\omega_\ell}\right)\right) E_\ell = 0 \tag{3.1.14}$$

4 Parametric Amplifier

We have seen that the nonlinear EP is typically associated with a kink in the lasing frequency and output power (at least for a small enough D1). However, even if the system is only near the EP, the previous trends are expected to persist, but the kinks are changed into smoother variations. We show here that we can characterize and confirm the EP using a scattering setup. In particular, we scatter light off the laser cavity using an infinitesimal external source at frequency ω_s with a detuning $\sigma = \omega_s - \omega_\ell$. We can compute the scattered field by linearizing the Maxwell–Bloch equation (7) around the lasing solution. In this limit, a degenerative four-wave mixing process occurs, leading to an idler field at frequency $\omega_i = 2\omega_\ell - \omega_s$. The fields can then be obtained by numerically solving the following coupled equations, where subscripts s and i refer to signal and idler fields (see details in the supplementary material):

$$\begin{aligned}
-i\omega_s \delta J_s &= \nabla^2 \delta E_s + \omega_s^2 \left[\epsilon_c + \frac{i\sigma_c}{\omega_s} + \Gamma_s D_\ell (1 + \alpha |E_\ell|^2)\right] \delta E_s + \omega_s^2 \Gamma_s D_\ell \beta E_\ell^2 \delta E_i^*, \\
\alpha &= \frac{\Gamma_s - \Gamma_\ell^*}{2(i + \frac{\sigma_c}{\gamma_\parallel}) + (\Gamma_i^* - \Gamma_s)|E_\ell|^2}, \\
0 &= \nabla^2 \delta E_i + \omega_i^2 \left[\epsilon_c + \frac{i\sigma_c}{\omega_i} + \Gamma_i D_\ell (1 + \beta^* |E_\ell|^2)\right] \delta E_i + \omega_i^2 \Gamma_i D_\ell \alpha^* E_\ell^2 \delta E_s^*, \\
\beta &= \frac{\Gamma_\ell - \Gamma_i^*}{2(i + \frac{\sigma_c}{\gamma_\parallel}) + (\Gamma_i^* - \Gamma_s)|E_\ell|^2}.
\end{aligned} \tag{13}$$

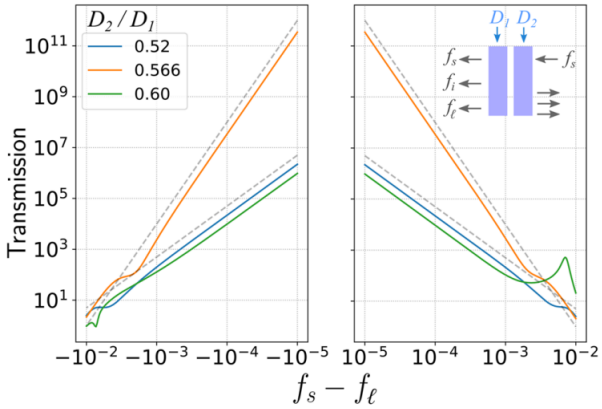

Figure 3: Transmission at the signal frequency f_s due to an infinitesimal source for different pump values $D2$ ($D1$ being fixed at 0.95) and $\frac{\gamma_\parallel a}{2\pi c} = 10^{-2}$. Results are obtained by numerically solving Eq. (14) using a finite difference scheme. The gray dashed line represents quadratic and quartic scaling rates. The EP laser ($\frac{D2}{D1} \approx 0.566$) is clearly associated with an inverse quartic variation of the transmitted intensity with detuning from the laser line.

4.1 Scattering Perturbation

We know that in a single-mode lasing solution E, P, and D satisfies

$$\nabla^2 E^+ = \ddot{P}^+ + \epsilon_c \ddot{E}^+ + \sigma_c \dot{E}^+ \tag{4.1.1}$$

$$i\dot{P}^+ = (\omega_a - i\gamma_\perp)P^+ + \gamma_\perp E^+ D \tag{4.1.2}$$

$$\dot{D}/\gamma_\parallel = D_0 - D + \mathrm{Im}(E^{*+} \cdot P^+) \tag{4.1.3}$$

We assume a single-mode lasing solution to the Maxwell-Bloch equations with a field $E_l(x,t) = E_l(x)e^{-i\omega_l t}$. We scatter light off the laser cavity with an infinitesimal external source $\delta J_s(x,t) = \delta J_s(x)e^{-i\omega_s t}$ at a frequency ω_s. We have $D = D_0 + \frac{1}{2i}(E_\ell^* \cdot P_\ell - E_\ell \cdot P_\ell^*)$ as we derived before.

Now we propose that the solution is of the form:

$$E + \delta E \tag{4.1.4}$$

$$P + \delta P \tag{4.1.5}$$

$$D + \delta D \tag{4.1.6}$$

To solve this problem, we linearise Maxwell-Bloch equations around the lasing solution, which gives

$$\nabla^2 \delta E = \delta\ddot{P} + \epsilon_c \delta\ddot{E} + \sigma_c \delta\dot{E} + \delta\dot{J} \tag{4.1.7}$$

$$\delta\dot{P} = -(i\omega_a + \gamma_\perp)\delta P - i\gamma_\perp(D_\ell \delta E + \delta D E_\ell) \tag{4.1.8}$$

$$\delta\dot{D} = -\gamma_\parallel \delta D + \frac{i\gamma_\parallel}{2}(\delta E P_\ell^* + E_\ell \delta P^* - \delta E^* P_\ell - E_\ell^* \delta P) \tag{4.1.9}$$

The presence of the nonlinear terms means that an idler field with frequency $\omega_i = 2\omega' - \omega_s$ will be generated. Using $\sigma = \omega_s - \omega'$, we consider solutions of the form:

$$\delta E = \delta E_s e^{-i\omega_s t} + \delta E_i e^{-i\omega_i t},\ \delta P = \delta P_s e^{-i\omega_s t} + \delta P_i e^{-i\omega_i t},\ \delta D = \delta D_s e^{-i\sigma t} + \delta D_i e^{i\sigma t}. \tag{4.1.10}$$

Note that since δD is real, $\delta D_i = \delta D_s^*$. Plugging in Eq. (S9) and equating each frequency component, for $m = \{s, i\}$ and $\Gamma_m = \Gamma(\omega_m)$, we have:

$$-i\omega_m \delta J_m = \nabla^2 \delta E_m + \omega_m^2 \delta P_m + \omega_m^2 \epsilon_c \delta E_m + i\omega_m \sigma_c \delta E_m \tag{4.1.11}$$

$$\delta P_m = \Gamma_m(D_\ell \delta E_m + \delta D_m E_\ell) \tag{4.1.12}$$

$$(\gamma_\parallel - \sigma)\delta D_s = \frac{i\gamma_\parallel}{2}(\delta E_s P_\ell^* + E_\ell \delta P_i^* - \delta E_i^* P_\ell - E_\ell^* \delta P_s) \tag{4.1.13}$$

Using the expression for δP_s and the fact that $P_\ell = \Gamma_\ell D_\ell E_\ell$, we can compute δD_s as:

$$-2(i + \sigma/\gamma_\parallel)\delta D_s = (\Gamma_i^* - \Gamma_s)|E_\ell|^2 \delta D_s + (\Gamma_\ell^* - \Gamma_s) D_\ell E_\ell^* \delta E_s + (\Gamma_i^* - \Gamma_\ell) D_\ell E_\ell \delta E_i^* \tag{4.1.14}$$

We can finally use this to compute δP_m as a function of the electric fields

$$\delta P_s = \Gamma_s D_\ell[(1 + \alpha|E_\ell|^2)\delta E_s + \beta E_\ell{}^2 \delta E_s^*],\ \delta P_i = \Gamma_i D_\ell[\alpha^*|E_\ell|^2 \delta E_s^* + (1 + \beta^*|E_\ell|^2)\delta E_i] \tag{4.1.15}$$

$$\alpha = \frac{\Gamma_s - \Gamma_\ell^*}{2(i + \frac{\sigma_c}{\gamma_\parallel}) + (\Gamma_i^* - \Gamma_s)|E_\ell|^2} \tag{4.1.16}$$

$$\beta = \frac{\Gamma_\ell - \Gamma_i^*}{2(i + \frac{\sigma_c}{\gamma_\parallel}) + (\Gamma_i^* - \Gamma_s)|E_\ell|^2} \tag{4.1.17}$$

We can finally plug in Eq. (S9) obtain coupled equations for δ_s and δ_i

$$-i\omega_s \delta J_s = \nabla^2 \delta E_s + \omega_s^2 \left[\epsilon_c + \frac{i\sigma_c}{\omega_s} + \Gamma_s D_\ell (1 + \alpha |E_\ell|^2)\right] \delta E_s + \omega_s^2 \Gamma_s D_\ell \beta E_\ell^2 \delta E_i^* \tag{4.1.18}$$

$$0 = \nabla^2 \delta E_i + \omega_i^2 \left[\epsilon_c + \frac{i\sigma_c}{\omega_i} + \Gamma_i D_\ell (1 + \beta^* |E_\ell|^2)\right] \delta E_i + \omega_i^2 \Gamma_i D_\ell \alpha^* E_\ell^2 \delta E_s^* \tag{4.1.19}$$

5 Conclusion

The results presented here describe the general properties of stable nonlinear EP lasers above threshold and represent general guidelines for experimental demonstration. It can also be relevant beyond optics, such as in nonlinear PT symmetric circuits recently considered for wireless power transfer.